Redox Biology 10 (2016) 274–284

Contents lists available at ScienceDirect

Redox Biology

journal homepage: www.elsevier.com/locate/redox

Research Paper

Tumor cells have decreased ability to metabolize H_2O_2: Implications for pharmacological ascorbate in cancer therapy

Claire M. Doskey[a], Visarut Buranasudja[a], Brett A. Wagner[b], Justin G. Wilkes[c], Juan Du[c], Joseph J. Cullen[b,c,d], Garry R. Buettner[a,b,*]

[a] Interdisciplinary Graduate Program in Human Toxicology, The University of Iowa, Iowa City, IA 52242, USA
[b] Free Radical & Radiation Biology Program in the Department of Radiation Oncology, The University of Iowa, Iowa City, IA 52242, USA
[c] Department of Surgery, The University of Iowa, Iowa City, IA 52242, USA
[d] Veterans Affairs Medical Center, Veterans Affairs Medical Center, Iowa City, IA 52246, USA

ABSTRACT

Ascorbate ($AscH^-$) functions as a versatile reducing agent. At pharmacological doses (P-$AscH^-$; [plasma $AscH^-$] ≥≈20 mM), achievable through intravenous delivery, oxidation of P-$AscH^-$ can produce a high flux of H_2O_2 in tumors. Catalase is the major enzyme for detoxifying high concentrations of H_2O_2. We hypothesize that sensitivity of tumor cells to P-$AscH^-$ compared to normal cells is due to their lower capacity to metabolize H_2O_2. Rate constants for removal of H_2O_2 (k_{cell}) and catalase activities were determined for 15 tumor and 10 normal cell lines of various tissue types. A differential in the capacity of cells to remove H_2O_2 was revealed, with the average k_{cell} for normal cells being twice that of tumor cells. The ED_{50} (50% clonogenic survival) of P-$AscH^-$ correlated directly with k_{cell} and catalase activity. Catalase activity could present a promising indicator of which tumors may respond to P-$AscH^-$.

1. Introduction

Ascorbate functions as a versatile reducing agent in biology. When present at healthy physiological concentrations (40–80 μM) it exhibits antioxidant properties. It is essential in maintaining the function of enzymes that have roles in cell signaling events, *i.e.* the prolyl hydroxylases. When used at pharmacological doses (P-$AscH^-$ plasma levels ≥≈20 mM),[1] which are well above those obtained through healthy dietary intake and can be achieved only through intravenous delivery, its oxidation can deliver a high flux of H_2O_2 [1–4]. This unique feature of P-$AscH^-$ is currently being investigated for use as an adjuvant to standard of care therapies for multiple cancers. Both *in vitro* and *in vivo* studies have shown a differential toxicity of P-$AscH^-$ across various cancer types and selective toxicity to cancer cells in comparison to normal cells of the same tissue origin [1,3,5–13]. These studies have implicated the H_2O_2 produced from the oxidation of P-$AscH^-$ as the principal mediating factor in its cytotoxicity to cancer cells. The differential sensitivity of cancer cells of different tissue types to P-$AscH^-$, as well as their increased sensitivity over normal cells may be due to differences in their ability to remove H_2O_2, which is a function of the activities of antioxidant enzymes that detoxify H_2O_2.

While H_2O_2 is a strong oxidant, it is not very reactive because of its slow reaction kinetics with the majority of biomolecules. Thus, it can accumulate to relatively high concentrations in cells and tissues. There it can be activated to produce more reactive oxidants, such as compound-I of heme peroxidases and hydroxyl free radicals. The removal of excess H_2O_2 by antioxidant enzymes is therefore central in minimizing cellular damage. The principal enzymes responsible for the elimination of H_2O_2 are catalase, glutathione peroxidase (GPx), and the peroxiredoxins (Prx) [14–17]. Kinetic models built using *in vitro* data have demonstrated that catalase is the major enzyme involved in the detoxification of high concentrations of H_2O_2, such as those that result from the oxidation of P-$AscH^-$ in the culture medium, whereas GPx and the Prxs are responsible for removing low fluxes of H_2O_2 [16,18–26]. Catalase is largely localized to the peroxisomes of nucleated mammalian cells where it catalyzes the decomposition of H_2O_2 into water and oxygen [27].

Biochemical studies of various tissues have shown that the endogenous levels of antioxidant enzymes differ greatly across tissue types [28]. It has been postulated that this reflects differences in development and metabolism across different organ systems [29]. The intrinsic levels of antioxidant enzymes are low in a majority of cancer

* Corresponding author at: Free Radical & Radiation Biology, Department of Radiation Oncology, Med Labs B180, The University of Iowa, Iowa City, IA 52242, USA.
E-mail address: garry-buettner@uiowa.edu (G.R. Buettner).

[1] **Abbreviations** 3-AT, 3-amino-1,2,4-triazole; $AscH^-$, ascorbate monoanion, *i.e.* vitamin C; ED_{50}, effective dose 50% survival; GPx, glutathione peroxidase; H_2O_2, hydrogen peroxide; P-$AscH^-$, pharmacological ascorbate; Prx, peroxiredoxins.

http://dx.doi.org/10.1016/j.redox.2016.10.010
Received 17 October 2016; Accepted 22 October 2016
Available online 28 October 2016

cell types as compared to non-transformed cells [28–30]. Studies have shown that all but one human cancer cell type, a human renal adenocarcinoma, have low levels of both catalase and GPx [29]. This suggests that the vast majority of cancer cells may lack the biochemical machinery needed to detoxify higher fluxes of H_2O_2 efficiently. While in general, the levels of catalase are low in cancer cells, catalase activity appears to vary greatly across different cancer cell lines [28]. This may correspond to a differential capacity to remove H_2O_2 and differential sensitivity to H_2O_2 -producing agents (*i.e.* P-AscH$^-$). We hypothesize that the sensitivity of tumor cells to P-AscH$^-$ compared to normal cells is due to their lower capacity to remove extracellular H_2O_2; across different tumor cell types there will also be a differential sensitivity to P-AscH$^-$ that is correlated with their individual capacities to remove extracellular H_2O_2, as reflected by k_{cell} of H_2O_2 removal and catalase activity.

2. Methods

2.1. Cell lines

MIA PaCa-2, PANC-1, AsPC-1, MB231, A549, FHs74int and HepG2 cells were purchased from American Type Culture Collection (Manassas, VA). Two patient-derived cell lines, 339 and 403, were obtained from Medical College of Wisconsin surgical oncology tissue bank (Milwaukee, WI) [31,32]. A375, Cal27, FaDu, H292, H1299, U87, U118, H6c7, melanocytes, normal human fibroblasts (NHF; 12 and 46 years old), normal human astrocytes (NHA), and HBePC cells were donated from neighboring labs and were only used in experiments to determine their rate constant for H_2O_2 removal. MIA PaCa-2, PANC-1, MB231, A549, and HepG2 cells were cultured in Dulbecco's modified eagle medium (DMEM) with high glucose from Invitrogen (Grand Island, NY), supplemented with 10% fetal bovine serum (FBS) and penicillin (80 Units mL^{-1})/streptomycin (80 μg mL^{-1}) at 37 °C, 5% CO_2. AsPC-1 cells were cultured in RPMI 1640 medium from Invitrogen (Grand Island, NY), supplemented with 10% FBS and penicillin (80 Units mL^{-1})/streptomycin (80 μg mL^{-1}) at 37 °C, 5% CO_2. 339 and 403 cells were cultured in DMEM nutrient mixture F-12 (Ham) medium from Invitrogen (Grand Island, NY), supplemented with 6% FBS, penicillin (80 Units mL^{-1})/streptomycin (80 μg mL^{-1}), 0.1% epidermal growth factor (EGF) human recombinant, 0.4% bovine pituitary extract, 4% hydrocortisone, 0.014% insulin human recombinant and GlutaMAX™ at 37 °C, 5% CO_2. Sufficient medium was prepared to complete an experiment, including all replicates and contained FBS from the same lot number to minimize variation between experiments.

2.2. Measurement of ascorbate oxidation in cell culture medium with Clark electrode oxygen monitor

The rate of oxygen consumption (OCR, -d[O_2]/dt) upon addition of ascorbate to DMEM cell culture medium complete with 10% FBS and penicillin (80 Units mL^{-1})/streptomycin (80 μg mL^{-1}) was determined using a Clark electrode oxygen monitor (YSI Inc.) that is connected to an ESA Biostat microelectrode system (ESA Products, Dionex Corp.). The OCR represents the rate of H_2O_2 production. The accumulation of H_2O_2 is determined with this system through the addition of catalase (500 units mL^{-1}) (bovine liver, Sigma C-1345).

2.3. H_2O_2 removal assay: determination of rate constant by which cells remove H_2O_2

The rate constant (k_{cell}) for the removal of extracellular H_2O_2 by cells was determined for each of the different cell lines using the 96-well plate reader assay [33]. Cells were seeded in rows E-G of a 96-well plate at a density of 15,000 cells per well. Cells were then incubated for 48 h prior to the assay at 37 °C, 5% CO_2 to return to a healthy exponential growth state. Briefly, extracellular H_2O_2 (10 μM) was added to wells at different times; the number of cells in the wells at the time of exposure was verified. The cells removed this extracellular H_2O_2 over time. The system was then quenched at a predetermined time and the concentration of extracellular H_2O_2 remaining in the wells was determined. The quenching solution contains horseradish peroxidase (HRP) that reacts with the remaining H_2O_2 in the wells. The activated HRP then oxidizes *para*-hydroxyphenylacetic acid (*p*HPA) resulting in the formation of the fluorescent *p*HPA dimer, providing the readout of the amount of H_2O_2 remaining in the wells. With this method an observed k_{cell} of H_2O_2 removal was determined on a per cell basis, *i.e.* the capacity of cells to remove extracellular H_2O_2 (k_{cell}).

2.4. Measurement of catalase activity

Catalase activity was measured in MB231, A549, HepG2, MIA PaCa-2, AsPC-1, PANC-1, 403, and 339 cell lysates using a spectrophotometric-based assay [34]. Briefly, cells (1.0–5.0×10^6) were harvested in 200 μL phosphate buffered saline (PBS). Cells were counted with the hemacytometer, so a well-defined number of cells was used in the assay. After cell lysis *via* sonication, the cell lysate was diluted in 50 mM phosphate buffer (pH 7.0) and 30 mM H_2O_2 was added to the cell lysate in the cuvette to yield a final concentration of 10 mM H_2O_2. The decomposition of H_2O_2 was followed by the decrease in absorbance at 240 nm measured every 10 s for 2 min. The effective number of active catalase monomers per cell was determined from the experimental slope, k', of a plot of ln(absorbance due to H_2O_2) *vs.* time (s). This experimental k', the number of cells used for the assay, information on all solution volumes and dilutions, along with the rate constant k=1.1×10^7 M^{-1} s^{-1} for the catalytic rate constant for the reaction of catalase monomer with H_2O_2 [35–38] were used to determine the number of catalase monomers per cell.

2.5. Inhibition of catalase with 3-Amino-1,2,4-triazole

Catalase was inhibited using 3-amino-1,2,4-triazole (3-AT). Cells were treated with 20 mM 3-AT for 1 h at 37 °C, 5% CO_2. Cells were then washed 3 times with PBS to remove extracellular 3-AT prior to being used for experiments described herein.

2.6. Transduction with adenovirus catalase

MIA PaCa-2 cells were plated 48 h prior to transduction. Complete DMEM medium was removed and cells were washed 2 times with serum-free DMEM medium. Cells were then transduced with adenovirus catalase (1×10^{10} pfu mL^{-1}) for 24 h at desired MOI (*i.e.* 1, 5, 10, 25, 50, and 100 for experiments herein) in serum-free DMEM medium. After 24 h, adenovirus catalase was removed and cells were washed with complete DMEM medium prior to replacement with complete DMEM medium for a 24-h incubation prior to being used for the experiments described herein.

2.7. Exposure to ascorbate

MIA PaCa-2, AsPC-1, PANC-1, 339, and 403 cells were seeded into multiple 60 mm^2 culture dishes at 250,000 cells per dish and were cultured for 48 h at 37 °C, 5% CO_2. One dish was used strictly for calculating the initial dose in units of mol cell^{-1}. To achieve this, prior to exposure to ascorbate, cells were counted in this dish with a hemocytometer; this number of total cells, which were present immediately prior to exposure, was used to calculate the initial dose in units of mol cell^{-1}. Growth medium was exchanged with DMEM high glucose medium with 10% FBS and penicillin (80 Units mL^{-1})/streptomycin (80 μg mL^{-1}) for all exposures to ascorbate. Subtle changes in the exposure-medium can result in different rates of oxidation of ascorbate and therefore differences in the flux of H_2O_2

the cells are exposed to. For these studies, all cells were exposed in DMEM high glucose medium with 10% FBS and penicillin (80 Units mL^{-1})/streptomycin (80 μg mL^{-1}). After the replacement with fresh DMEM high glucose complete medium (3.0 mL), ascorbate was added to medium to achieve exposures of 0–150 picomoles $cell^{-1}$ (pico =10^{-12}; abbreviation = pmol $cell^{-1}$), *i.e.* 0–8 mM. For control experiments, medium was replaced with fresh DMEM high glucose medium, but cells were untreated. Cells were then incubated for 1 h at 37 °C, 5% CO_2.

2.8. Clonogenic cell survival

To assess the cytotoxicity of exposure to P-$AscH^-$, cells were plated for a clonogenic assay following the 1-h exposure to ascorbate. The exposure medium was removed, cells trypsinized and counted with a hemocytometer and plated at a cell density of 500 cells in 3.0 mL of medium in 60 mm^2 dishes. Plates were incubated for 11–14 days at 37 °C, 5% CO_2. After the growth period, cells were fixed with 70% ethanol and stained with Coomassie Blue. Colonies were counted as a grouping of 50 or more cells. The plating efficiency and surviving fraction were determined; plating efficiency (PE) =(colonies counted/cells plated)×100; survival fraction =(PE of treated sample / PE of control)×100. From plots of clonogenic survival fraction *vs.* dose of ascorbate, the Effective Dose for 50% clonogenic survival (ED_{50}) was determined.

2.9. Measurement of intracellular ATP concentration

A cell suspension (100 μL, 50,000 cells) was added to each well in an opaque-walled, 96-well plate. To this, 100 μL of reagent from an ATP kit (Promega, CellTiterGlo) was added to lyse the cells and initiate the luminescence reaction. After 10 min, luminescence was measured on a microplate reader. ATP standard curves with concentrations between 0 and 1000 μM were generated for each experiment. The ATP concentration was determined from the corresponding standard curve and converted to an intracellular concentration using the cell number as counted on a hemocytometer; cell volume as measured with the Moxi automated cell counter (ORFLO™).

2.10. Genomic DNA isolation and quantitative PCR (QPCR)

Genomic DNA was isolated using Blood & Cell Culture DNA Mini Kit (Qiagen, Valencia, CA) as described by the manufacturer. Genomic DNA isolation by this technique has been demonstrated to be suitable for QPCR-based measurement of both nuclear DNA (nDNA) and mitochondrial DNA (mtDNA) damage without a separate step for mitochondrial DNA purification [39]. The QPCR analysis of DNA damage is based on the principle that various types of DNA lesions can slow or impede the progression of DNA polymerase. If equal amounts of DNA from different biological samples are amplified under identical PCR conditions, DNA with more damage will amplify to a lesser extent than DNA with less damage. Hence, the amount of PCR amplification is inversely proportional to lesion frequency within a given DNA sample.

Prior to QPCR, concentrations of total cellular DNA were quantified with the Implen Nanophotometer P-330 at 260 nm. QPCR was performed in a 2720 Thermal Cycle (Applied Biosystems, Foster City, CA) with LA PCR Kit, Version 2.1 (Clontech Laboratories, Mountain View, CA). The total volume of reaction was 50 μL, containing 15 ng (nDNA assay), or 5 ng (mtDNA assay) of total genomic DNA, 1X LA PCR buffer II (Mg^{2+} plus), 400 μM dNTP mixture, 0.4 μM primers and 2.5 units of Takara LA Taq. The oligonucleotide primers used in this study were prepared by Integrated DNA Technologies (Coralville, IA). The primer nucleotide sequences were as presented in [39]. The 12.2 kb region of the DNA polymerase beta gene was used to study nDNA lesions. The PCR conditions were: an initial denaturation at 94 °C for 2 min followed by 26 cycles of denaturation at 94.5 °C for 25 s, primer extension at 68 °C for 13 min (for nDNA) or 20 cycles of denaturation at 94 °C for 25 s, primer extension at 68 °C for 10 min 30 s (for mtDNA). A final extension at 72 °C was performed for 10 min at the end of PCR cycle. Fifty-percent controls, containing half of the amount of undamaged DNA, were used as a quality control for each PCR to validate that PCR reaction had been terminated within exponential phase. The PCR amplicons were quantified by fluorescence measurement with Quant-iT PicoGreen dsDNA Assay Kit (Invitrogen, Carlsbad, CA) according to the manufacturer. The specificities of PCR reactions were confirmed with agarose gel electrophoresis. Mitochondrial DNA amplifications of each sample were normalized with relative mitochondrial DNA copy number by standardizing to the amplification of small mitochondrial fragment (220 bp). DNA lesion frequencies were calculated as previously described [39–41], by the formula $\lambda = -\ln(A_D/A_{Ct})$, where λ= lesion frequency per fragment, A_D = amplification of treatment, A_{Ct} = amplification of control.

2.11. Animal experiments

Thirty-day-old athymic nude mice were obtained from Harlan Sprague-Dawley (Indianapolis, IN). The nude mice protocol was reviewed and approved by the Animal Care and Use Committee of The University of Iowa. The animals were housed four to a cage and fed a sterile commercial stock diet and tap water, *ad libitum*. Animals were allowed to acclimate in the unit for one week before any manipulations were performed. Each experimental group consisted of 4 mice, 2 tumors in each mouse. MIA PaCa-2 or PANC-1 human pancreatic tumor cells (2×10^6) were delivered subcutaneously into the flank region of nude mice with a 1-mL tuberculin syringe equipped with a 25-gauge needle. The tumors were allowed to grow until they reached between 3 mm and 4 mm in greatest dimension (2 weeks), at which time the mice were randomized and treatment was initiated. This was defined as day-1 of the experiment. Mice were treated with IP ascorbate (4 g/kg) twice daily for two weeks. Tumors were measured on day 3, 7, 10, and 14 following first treatment with ascorbate. Tumor size was measured using a digital caliper, and tumor volume was estimated according to: tumor volume =½×L×W^2, where L is the greatest dimension of the tumor, and W is the dimension of the tumor in the perpendicular direction [42]. Animals were euthanized by CO_2 asphyxiation when the tumors reached a predetermined size of 1000 mm^3 or at day-15.

2.12. Immunofluorescent staining of catalase in tumor tissue

Tumor samples were fixed with 4% paraformaldehyde at 4 °C overnight. Dry OCT sections of tumor were washed with PBS before blocking with 5% goat serum for 30 min at 20 °C. The tumor samples were incubated with catalase antibody (1:50, abcam, ab16731) for 20 h at 4 °C. An Alexa Fluor 488 nm goat anti-Rabbit (1:200) was used as secondary antibody. DAPI was used to stain the cell nuclei. Tumor tissue samples were examined with a confocal microscope (Zeiss LSM 710). The intensity of immunofluorescence was quantified using ImageJ.

2.13. Statistics

Statistical analysis was done using GraphPad Prism 6.04 software (GraphPad Software, San Diego, CA). Statistical significance was determined using two-tailed unpaired *t*- test **(**Fig. 1**)** and one-way ANOVA with Tukey post-test (Fig. 7). Error bars indicate standard error of the mean.

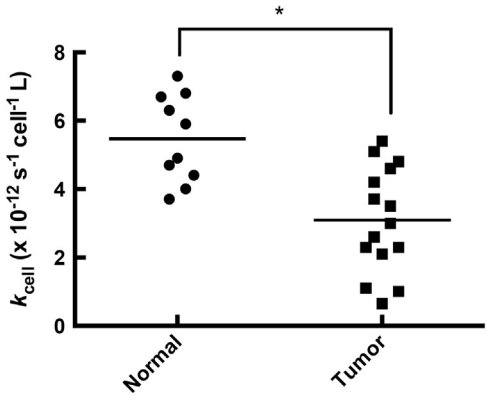

Fig. 1. Normal cells have a more robust capacity to remove extracellular H_2O_2 than tumor cells. The rate constants, k_{cell}, at which 10 normal cell lines and 15 cancer cell lines remove H_2O_2 were measured (listed in Table 1). There was a wide range of capacities for removal of H_2O_2 across all cell types. On average, normal cells had a 2-fold higher rate constant for the removal of H_2O_2 than tumor cells ($p < 0.05$).

3. Results

3.1. Pharmacological ascorbate is oxidized in cell culture medium

Oxidation of P-AscH$^-$ in both *in vitro* and *in vivo* settings generates a flux of H_2O_2 [2–4]. This flux of H_2O_2 is proposed to mediate the cytotoxicity of P-AscH$^-$ to cancer cells. The rate of oxygen consumption (OCR, -d[O_2]/d*t*) upon addition of P-AscH$^-$ to DMEM cell culture medium provides information on the flux of H_2O_2 [3,4] (Supplementary Fig. S1). Addition of P-AscH$^-$ (6.0 mM) to DMEM cell culture medium complete with 10% FBS resulted in an increase in the background rate of oxygen consumption rate of approximately 50 nmol L^{-1} s^{-1}, which represents the rate of H_2O_2 production from the oxidation of ascorbate. Addition of catalase indicated an accumulation of 18 μM H_2O_2 in the medium over the course of an experiment (Supplementary Fig. S1). In a typical experimental setting in which 125,000 cells were treated with 6.0 mM P-AscH$^-$ in 3.0 mL of DMEM medium, this would result in the cells being exposed to a 1.2 fmol $cell^{-1}$ s^{-1} flux of H_2O_2. The metabolic rate of oxygen consumption by low passage MIA PaCa-2 cells is on the order of 40 amol $cell^{-1}$ s^{-1} [43]. If we assume that a generous 1% of this metabolic oxygen consumption were to be converted to H_2O_2 [44], then the metabolic rate of production of H_2O_2 would be 0.4 amol $cell^{-1}$ s^{-1}, a very small fraction (1%) of the flux generated by the oxidation of ascorbate in the experiment. We have previously shown that the extracellular flux of H_2O_2 generated by the P-AscH$^-$ in the medium will increase the intracellular steady-state levels of H_2O_2 [45].

3.2. Normal cells have higher capacities for the removal of H_2O_2 in comparison to tumor cells

Rate constants (k_{cell}, [33]) for removal of extracellular H_2O_2 were measured for multiple cancer cells and normal cells, representing a variety of tissue types (*i.e.* skin, breast, pancreas, lung, tongue, pharynx, liver, and intestine). Results showed that both cancer cells and normal cells have a wide range of capacities to remove extracellular H_2O_2 (Table 1, Fig. 1). Overall there was an 11-fold difference in the k_{cell} for the removal of H_2O_2 when comparing the cell line with the lowest k_{cell} (A375; 0.65×10^{-12} s^{-1} $cell^{-1}$ L) to the cell line with the highest k_{cell} (normal human astrocytes; 7.3×10^{-12} s^{-1} $cell^{-1}$ L). On average normal cells have higher rate constants for removal of extracellular H_2O_2 in comparison to cancer cells, k_{cell} =5.5×10^{-12} s^{-1} $cell^{-1}$ L and 3.1×10^{-12} s^{-1} $cell^{-1}$ L, respectively (Fig. 1). Even among cancer cells from the same anatomical location, there was a considerable difference in k_{cell} for removal of extracellular H_2O_2 (Table 1). For example, MIA PaCa-2 cells have a small k_{cell} (1.1×10^{-12} s^{-1} $cell^{-1}$ L) while both the PANC-1 and 339 cells have large values for k_{cell}, 5.1×10^{-12} s^{-1} $cell^{-1}$ L and 5.4×10^{-12} s^{-1} $cell^{-1}$ L, respectively (Table 1).

Table 1
Rate Constants (k_{cell}) for H_2O_2 removal by tumor and normal cells.

Cell Line	Cell type	k_{cell} (10^{-12} s^{-1} $cell^{-1}$ L) (SEM)
Tumor		
MIA PaCa–2	Pancreatic Cancer	1.1 (0.1)
AsPC–1		2.6 (0.9)
PANC–1		5.1 (1.1)
339		5.4 (0.7)
403		3.5 (0.3)
A375	Melanoma	0.65 (0.21)
Cal27	Head and neck	2.3 (0.6)
FaDu	cancer	2.3
HepG2	Liver Cancer	4.2 (0.6)
MB231	Breast Cancer	1
H292	Lung Cancer	3.0 (0.4)
H1299		3.7 (0.4)
A549		2.1 (0.3)
U87	Glioblastoma	4.8 (0.6)
U118		4.6 (0.3)
Normal		
H6c7	Pancreas	3.7 (0.4)
Melanocytes	Skin	6.3 (1.3)
Normal Human Fibroblasts (12-y)		5.9
Normal Human Fibroblast (46-y)		4.7 (0.8)
Normal Human Astrocytes (#1)	Brain	6.8 (0.7)
Normal Human Astrocytes (#2)		4.4 (0.3)
Normal Human Astrocytes (#3)		7.3 (0.2)
HBePC	Lung	6.7 (0.6)
Red blood cells	Blood	4.0
FHs74int	Intestinal	4.9

3.3. Catalase activity varies across tumor cell lines and plays a major role in the removal of extracellular H_2O_2

Given the wide-range observed in the ability of different cancer cell lines to remove H_2O_2, it is expected that the activities of antioxidant enzymes involved in the metabolism of H_2O_2 will also vary greatly. Kinetic models indicate that catalase is the major antioxidant enzyme involved in the removal of H_2O_2 at concentrations greater than 10 μM, leading us to investigate the catalase activity in the tumor cell lines [21,22,24]. Similar to the observed variation in k_{cell} for removal of H_2O_2, we observed that cancer cells of varying tissue origins exhibit a wide range of catalase activity (Fig. 2A). This variation in the active catalase monomers per cell was also observed across cell lines of the same tissue type and was exemplified in the pancreatic cancer cell lines investigated (Fig. 2A). As expected, the number of active catalase monomers per cell correlated with the rate constants at which these cell lines remove extracellular H_2O_2 (Fig. 2B). Since catalase is the major contributing enzyme in the removal of high concentrations of H_2O_2, *e.g.* extracellular H_2O_2, it is not surprising that there is a strong correlation (R^2 =0.88) between these two parameters in the cell lines.

The data presented in Fig. 2B show a saturation behavior. This is as expected; if catalase levels in cells are high, then addition of more will lead to only a small increase in the ability of cells to remove H_2O_2; but if catalase levels are low, that same addition will lead to a relatively large increase in the ability of cells to remove H_2O_2, as manifest in k_{cell}. A similar saturation behavior on the mitochondrial flux of superoxide and rate of formation of H_2O_2 has been observed as the levels of MnSOD are varied in cells [46]. k_{cell} also incorporates the effects of the latency of catalase activity, whereas the results of the standard assay for

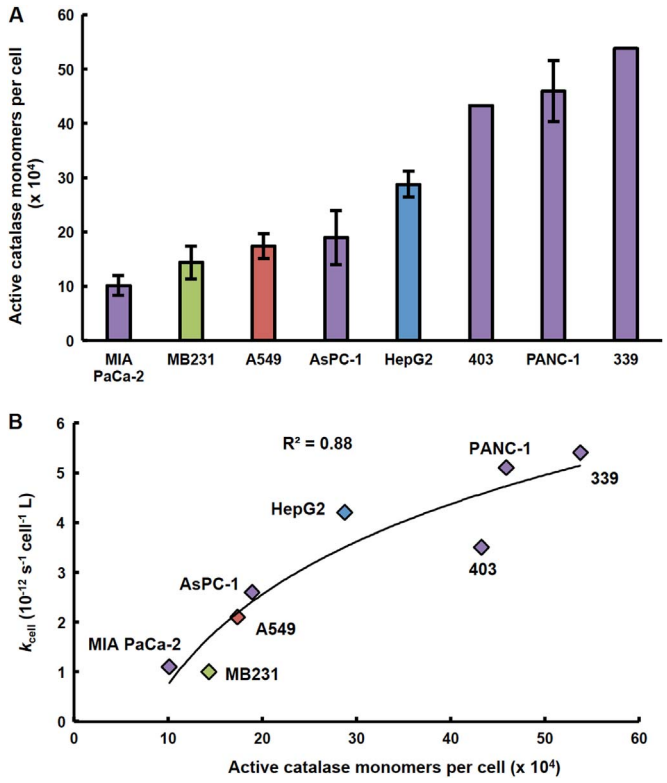

Fig. 2. Catalase activity varies across cancer cell lines and correlates with the rate constant for removal of H_2O_2 (k_{cell}). (A) Catalase activity for cell lines of different tissue origins (*i.e.* pancreas (purple), breast (green), lung (red), and liver (blue)) were determined and used to calculate the effective number of fully active catalase monomers per cell. This number varied 5-fold across the different cancer cell lines: from 101,000 monomers per cell (MIA PaCa-2) to 538,000 monomers per cell (339) (n =3–9, error bars are standard error of the mean). **(B)** There is a strong correlation between the rate constant at which these cell lines remove extracellular H_2O_2 and the effective number of fully active catalase molecules per cell (R^2 =0.88). (For interpretation of the references to color in this figure legend, the reader is referred to the web version of this article.)

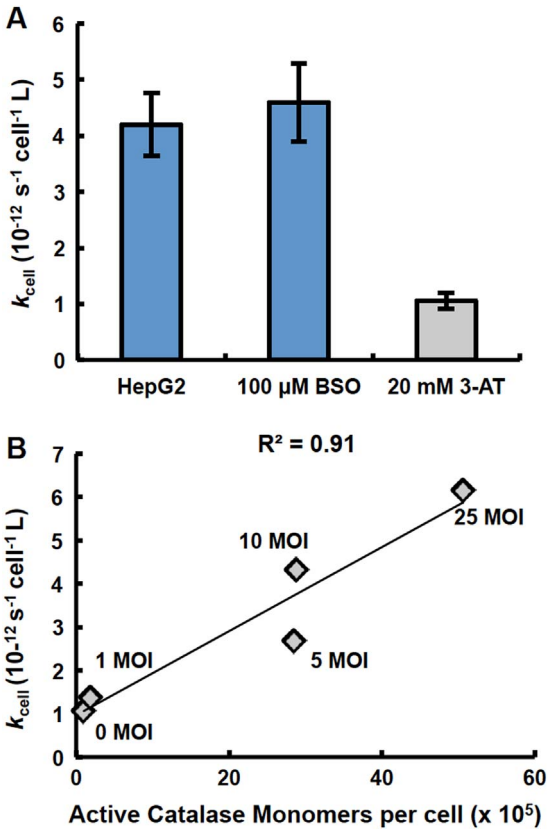

Fig. 3. Catalase plays a major role in removal of H_2O_2. (A) Treatment of HepG2 cells with 100 µM buthionine sulfoximine (BSO) 24 h prior to the H_2O_2-removal assay to inhibit glutathione synthesis did not result in any change in the rate constant by which these cells remove H_2O_2. However, treatment of HepG2 cells with 20 mM 3-AT for 1 h to inhibit catalase resulted in a four-fold decrease in the rate constant by which HepG2 cells remove extracellular H_2O_2 (n =4, error bars are standard error of the mean). **(B)** There is a direct correlation between the number of active catalase molecules per cell and the rate constant for removal of H_2O_2 following transduction of MIA PaCa-2 cells with adenovirus catalase (0–25 MOI) (R^2 =0.91).

catalase can overestimate the effective activity that may be present in intact cells [47].

When catalase was inhibited using 3-amino-1,2,4-triazole (3-AT) in HepG2 cells, which have a high basal level of catalase activity, there was a 4.6-fold decrease in the rate constant at which these cells remove extracellular H_2O_2 (Fig. 3A). These results both suggest and support the important role of catalase in the removal of high concentrations of extracellular H_2O_2. The number of active catalase molecules per cell, assessed from the measurement of catalase activity in HepG2 cells following inhibition of catalase with 3-AT, decreased 4.6-fold (Supplementary Fig. S2). This decrease in catalase activity mirrors the decrease in the rate constant, k_{cell}, for extracellular H_2O_2 removal (Fig. 3A and Supplementary Fig. S2).

Conversely, MIA PaCa-2 cells, which have a very low basal capacity to remove H_2O_2 (k_{cell}) and a markedly low catalase activity, were transduced with varying amounts (multiplicity of infection; MOI) of adenovirus catalase to produce sets of cells with a range of increased catalase activity. Following transduction, the rate constant at which these sets of MIA PaCa-2 cells remove H_2O_2 increased 1.5- to 80-fold (Supplementary Fig. S3A). The rate constants for the removal of H_2O_2 correlated directly with the resulting active catalase monomers per cell (Fig. 3B).

3.4. Dose of pharmacological ascorbate is best specified on a per cell basis

We have previously demonstrated that specifying applied dose of a xenobiotic (*i.e.* 1,4-benzoquinone, oligomycin A, and H_2O_2) in cell culture studies as moles of xenobiotic per cell, rather than initial concentration in the medium, yields more consistent results and reduces ambiguity across different physical experimental set-ups [48]. Oxidation of P-AscH$^-$ in both *in vitro* (*i.e.* in cell culture medium) and *in vivo* settings generates a flux of H_2O_2 [1–4]. The toxicity of H_2O_2 results in both irreversible and reversible changes to biomolecules and has been shown to be cell density dependent [49–51]. The dose of P-AscH$^-$ used in cell culture studies is currently reported in terms of its initial concentration in the medium. Data presented in Fig. 4 demonstrate that specifying dose as moles P-AscH$^-$ per number of cells exposed, yields more consistent results and reduces ambiguity. When P-AscH$^-$ is specified as moles per cell a clear dose response is observed (Fig. 4B), whereas expression of dose as the initial concentration in the medium produces ambiguous results when different physical set-ups (*e.g.* different number of cells exposed) are used (Fig. 4A).

3.5. The differential sensitivity to ascorbate across pancreatic cancer cell lines correlates with their capacity to remove H_2O_2

Previous studies have indicated that there is a range for the sensitivity of cancer cells to P-AscH$^-$ *in vitro* across different tissue types [1,3,6]. This is also demonstrated within the same tissues of origin. Five different pancreatic cancer cell lines, MIA PaCa-2, AsPC-1, 403, 339, and PANC-1, had a differential sensitivity to P-AscH$^-$ as measured by the dose that was effective in killing 50% of the cells *in*

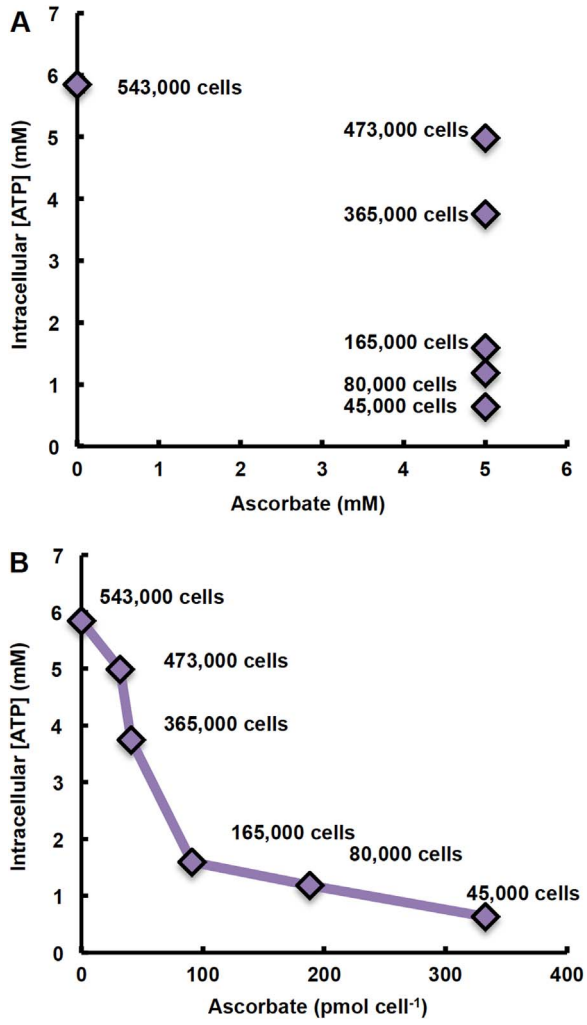

Fig. 4. Dose of ascorbate is better specified on a per cell basis (pmol cell^{-1}) than as initial concentration in the medium (mM). MIA PaCa-2 cells at varying cell densities (45,000–543,000 cells/3.0 mL medium) were treated with 5 mM ascorbate 1 h; ATP was measured immediately after. Dose of ascorbate is expressed as: **(A)** initial concentration of ascorbate in the medium; and **(B)** absolute amount of ascorbate (pmol) per cell.

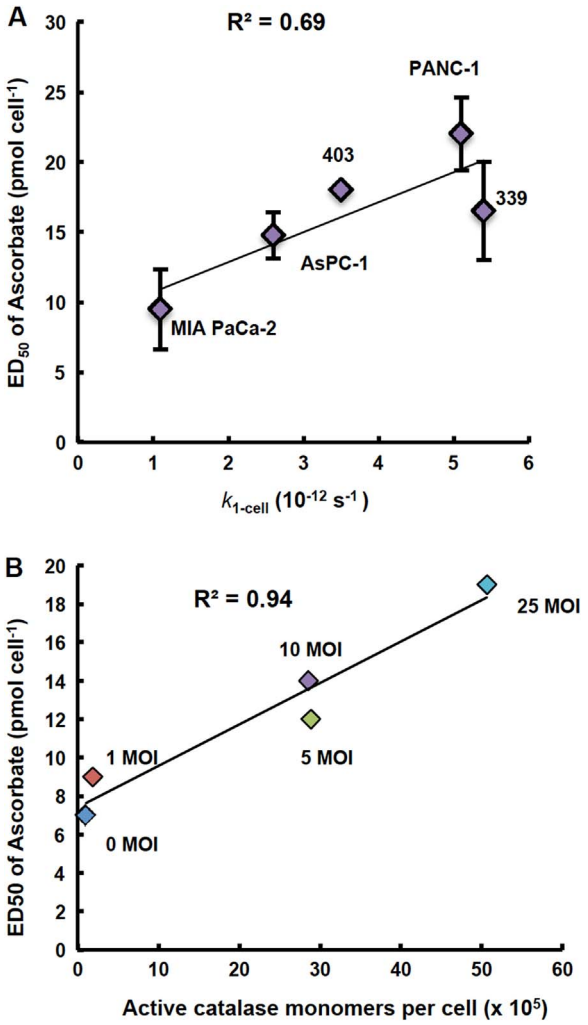

Fig. 5. Sensitivity to ascorbate varies across pancreatic cancer cell lines and correlates with the capacity to remove extracellular H_2O_2 ($k_{1\text{-cell}}$). (A) The ED_{50} of ascorbate was determined in MIA PaCa-2, AsPC-1, 403, 339, and PANC-1 cell lines using a clonogenic survival assay. The dose of ascorbate needed to decrease clonogenic survival by 50% varied across pancreatic cancer cell lines. When the rate constants for removal of extracellular H_2O_2 by a cell ($k_{1\text{-cell}}$) for these 5 different pancreatic cancer cell lines are plotted against the ED_{50} of P-AscH$^-$ there is a direct correlation between sensitivity to P-AscH$^-$ and the rate at which cells remove H_2O_2 (R^2 =0.69). The rate constant $k_{1\text{-cell}}$ represents the capacity of a single cell to remove extracellular H_2O_2. It is determined by: $k_{1\text{-cell}}$ (s^{-1}) = k_{cell} (s^{-1} $cell^{-1}$ L) x 1 (cell L^{-1}). **(B)** Transduction of MIA PaCa-2 cells with adenovirus catalase at increasing MOIs increases resistance to ascorbate as seen by ED_{50}. MIA PaCa-2 cells were transduced with adenovirus catalase at 0–25 MOI and then exposed to ascorbate (0–50 pmol cell^{-1}). The dose that decreased clonogenic survival by 50% was determined at each transduction-MOI of adenovirus catalase (0–25 MOI). Catalase activity was measured after transduction with adenovirus catalase. The resulting ED_{50} correlated with catalase activity at varying MOI of adenovirus catalase (R^2 =0.94).

vitro (ED_{50}) (Fig. 5A and Supplementary Fig. S4). PANC-1 cells had an ED_{50} of P-AscH$^-$ that was two times greater than MIA PaCa-2 cells, showing that MIA PaCa-2 cells were significantly more sensitive to P-AscH$^-$ than PANC-1 cells (Fig. 5A and Supplementary Fig. S4).

These pancreatic cancer cell lines have very different capacities to remove extracellular H_2O_2, as quantitatively represented by k_{cell} as well as the catalase activity of the cell lines (Table 1 and Fig. 2). The ED_{50} of P-AscH$^-$ correlated directly with k_{cell} (R^2 =0.69, Fig. 5A). MIA PaCa-2 cells were most sensitive to P-AscH$^-$ and had the smallest k_{cell}, whereas PANC-1 cells were the least sensitive to P-AscH$^-$ and had the largest k_{cell} (Fig. 5A). These results, showing strong correlations between the ability of cells to remove extracellular H_2O_2 and ED_{50} of P-AscH$^-$, support the important role of the H_2O_2-removal system in the resulting toxicity observed from P-AscH$^-$. P-AscH$^-$ may be more effective in cells that have a lower capacity to remove H_2O_2. The strong correlation between catalase activity and sensitivity to P-AscH$^-$, as well as the effect of 3-AT inhibition of catalase on k_{cell} emphasize the role of catalase in the removal of H_2O_2 at high concentrations, such as those achievable by P-AscH$^-$.

Across different pancreatic cancer cell lines, we observed a strong correlation between k_{cell} and their sensitivity to P-AscH$^-$, so we explored this further in MIA PaCa-2 cells following transduction with adenovirus catalase at varying MOIs (0–25 MOI) (Fig. 5B and Supplementary Fig. S5). We saw a shift in the dose-response curve following treatment with P-AscH$^-$ that was MOI-dependent (Supplementary Fig. S5). The dose of P-AscH$^-$ that decreased clonogenic survival by 50% (ED_{50}) very strongly correlated with the catalase activity resulting from the transduction of varying MOIs of adenovirus catalase (R^2 =0.94) (Fig. 5B).

3.6. Inhibition of catalase sensitizes PANC-1 cells to pharmacological ascorbate

Catalase varies across tumor cell lines and plays a major role in the removal of H_2O_2 at concentrations comparable to those generated by P-

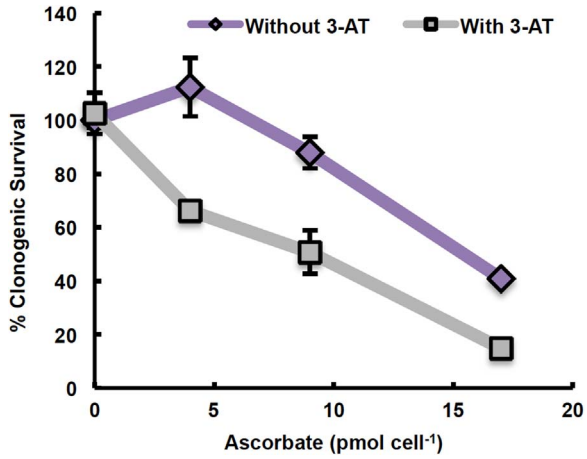

Fig. 6. Inhibition of catalase with 3-amino-1,2,4-triazole sensitizes PANC-1 cells to ascorbate parallels the decrease in k_{cell}. PANC-1 cells were treated with 20 mM 3-AT for 1 h prior to treatment with 0–17 pmol cell^{-1} ascorbate (350,000 cells; 0–2 mM) for 1 h. Cells were then plated for a clonogenic survival assay. 3-AT sensitized PANC-1 cells to ascorbate. The ED_{50} of ascorbate was 1.5-fold less with 3-AT treatment than without (n =3, error bars are standard error of the mean).

$AscH^-$ (Figs. 2 and 3). The ability of the different pancreatic cancer cell lines to remove H_2O_2, quantified *via* k_{cell}, correlated with the ED_{50} for P-$AscH^-$ in cell culture, with PANC-1 cells being the most resistant to P-$AscH^-$ and having the most robust capacity to remove extracellular H_2O_2 (Fig. 5A). When catalase was inhibited with 3-AT in PANC-1 cells prior to treatment with P-$AscH^-$, the cells were sensitized to P-$AscH^-$ (Fig. 6). The dose of P-$AscH^-$ needed to decrease clonogenic survival by 50% was 1.5-fold less when cells were pretreated with 3-AT (Fig. 6). Pretreatment with 3-AT resulted in a 40% reduction in the rate constant at which PANC-1 cells remove H_2O_2 (Supplementary Fig. S6A) and a 60% decrease in catalase activity (Supplementary Fig. S6B).

3.7. P-$AscH^-$ induces DNA damage and depletion of ATP via H_2O_2

As a macromolecule, DNA is vulnerable to oxidative damage induced by P-$AscH^-$ [52]. Treatment of MIA PaCa-2 cells with P-$AscH^-$ resulted in DNA damage to both nuclear DNA (nDNA) and mitochondrial DNA (mtDNA) in a dose-dependent manner (Fig. 7A). The frequency of lesions in mtDNA was approximately 3 times greater than in nDNA at doses of P-$AscH^-$ of 14 and 28 pmol cell^{-1} (Fig. 7A). This observation suggests that mtDNA is more susceptible to oxidative damage caused by P-$AscH^-$, compared to nDNA. To investigate whether H_2O_2 mediates the DNA damage observed upon exposure to P-$AscH^-$, MIA PaCa-2 were co-treated with P-$AscH^-$ (14 pmol cell^{-1}) and extracellular catalase (200 units mL^{-1}). Catalase ameliorated the detrimental effect of P-$AscH^-$ on both nDNA and mtDNA, consistent with the involvement of H_2O_2 in DNA damage mediated by P-$AscH^-$ (Fig. 7A and B).

The response to DNA damage is closely associated with depletion of ATP [53,54]. It has previously been observed that P-$AscH^-$ can result in the loss of intracellular ATP [1,3,10,55,56]. P-$AscH^-$ decreased the intracellular concentration of ATP in a dose-dependent manner (Fig. 4). Catalase prevented this depletion of ATP (Fig. 7C). These results clearly indicate that H_2O_2 plays an important role in ascorbate-mediated ATP depletion. The combination of DNA damage coupled with compromised levels of ATP due to the H_2O_2 produced by P-$AscH^-$ is detrimental to cancer cells – inhibiting growth or inducing cell death, depending on the severity of challenge.

3.8. Pharmacological ascorbate has increased efficacy in treating MIA PaCa-2 tumors in comparison to PANC-1 tumors in vivo

To determine if the differential sensitivity to P-$AscH^-$ observed in cell culture for MIA PaCa-2 and PANC-1 cells also occurs *in vivo*, a mouse model was used. Mouse xenografts of MIA PaCa-2 (k_{cell} =1.1×10^{-12} s^{-1} cell^{-1} L; 101,000 active catalase monomers per cell) and PANC-1 (k_{cell} =5.1×10^{-12} s^{-1} cell^{-1} L; 459,000 active catalase monomers per cell) cells were established; then, the mice were treated with P-$AscH^-$ IP twice daily for 2 weeks (Fig. 8). P-$AscH^-$ decreased tumor growth for both cell types in comparison to untreated controls. However, P-$AscH^-$ showed a greater inhibition of tumor growth for MIA PaCa-2 xenografts in comparison to PANC-1 xenografts, consistent with our *in vitro* observations (Fig. 8). The growth rate of the MIA PaCa-2 tumors in the untreated control group resulted in a 30% increase in tumor size per day compared to only a 2.7% increase in size each day for the MIA PaCa-2 tumors treated with P-$AscH^-$. The growth rate of the PANC-1 tumors in the untreated control group gave a 50% increase in tumor size per day compared to 21% increase per day for the PANC-1 tumors treated with P-$AscH^-$ (Fig. 8). Thus, P-$AscH^-$ brought about a 10-fold decrease in the rate of growth for tumors formed from MIA PaCa-2 cells while P-$AscH^-$ was only able to produce a 60% reduction in the rate of tumor growth for tumors derived from PANC-1 cells. The fluorescent intensity of PANC-1 *vs.* MIA PaCA-2 is approximately 50:1, indicating more catalase in the PANC-1-derived tissue samples (Fig. 8). These data suggest that the reduced ability of tumor tissue to remove H_2O_2 *in vivo* is a fundamental aspect of the mechanism by which P-$AscH^-$ slows tumor growth.

4. Discussion

The data presented here quantitatively establish a central role for H_2O_2, generated upon the oxidation of P-$AscH^-$, in the cytotoxic effects of P-$AscH^-$ to cancer cells *in vitro*. Our data quantitatively support the many observations that indicate that the cytotoxicity of P-$AscH^-$ to cancer cells observed *in vitro* is largely due to its generation of H_2O_2 in the medium (Supplementary Fig. S1) [1–5,9]. Ascorbate delivered at pharmacological concentrations has shown selective toxicity to several different tumor cell types. While this selective cytotoxicity has been observed to be dependent on the generation of H_2O_2, the mechanism by which this occurs is still under investigation. Several mechanisms for how the H_2O_2 generated by P-$AscH^-$ elicits its cytotoxicity to tumor cells have been hypothesized and examined, for example: DNA damage [3,13,52,55–57]; and the depletion of ATP leading to tumor cell death [1,3,10,58,59]. H_2O_2 plays an integral role in the mechanism. However, many other factors can modulate the toxicity of P-$AscH^-$, *e.g. KRAS* status [3], the level of catalytic metals [60,61], the redox status of the intracellular GSSG,2 H^+/2GSH redox couple [45,62], and the status of NAD [58]. Yun et al. recently extended the observations that ascorbate selectively kills *KRAS* and *BRAF* mutant cells [59]; they suggest that P-$AscH^-$ has as a target the redox state of GAPDH. However, the mechanism the authors propose does not consider important published data that clearly demonstrate that P-$AscH^-$ induces selective oxidative stress and cytotoxicity in cancer cells *vs.* normal cells by a mechanism involving the production of H_2O_2. Some of the biochemical reagents used to probe possible mechanism react directly with H_2O_2, thereby removing it and protecting the cells; see Supplementary Discussion.

There is a wide-range of abilities that different tissue types remove H_2O_2. We quantitatively determined such capacities for 10 different normal tissue cell types and 15 different cancer cell lines (Table 1). On average, the normal cells measured removed H_2O_2 with a rate constant that was 2-fold higher than the cancer cell lines tested (Table 1 and Fig. 1). We observed a large range in these rate constants of removal of H_2O_2 both across different tissue types and within different cell lines of the same tissue origin (Table 1).

In particular, there was a wide-range of k_{cell} for removal of H_2O_2 across the different pancreatic cancer cell lines (5-fold) (Table 1 and Fig. 2A). P-$AscH^-$ has been studied extensively in the pancreatic cancer model *in vitro*, *in vivo*, and in clinical trials [3,4,8,63,64]. Utilizing the

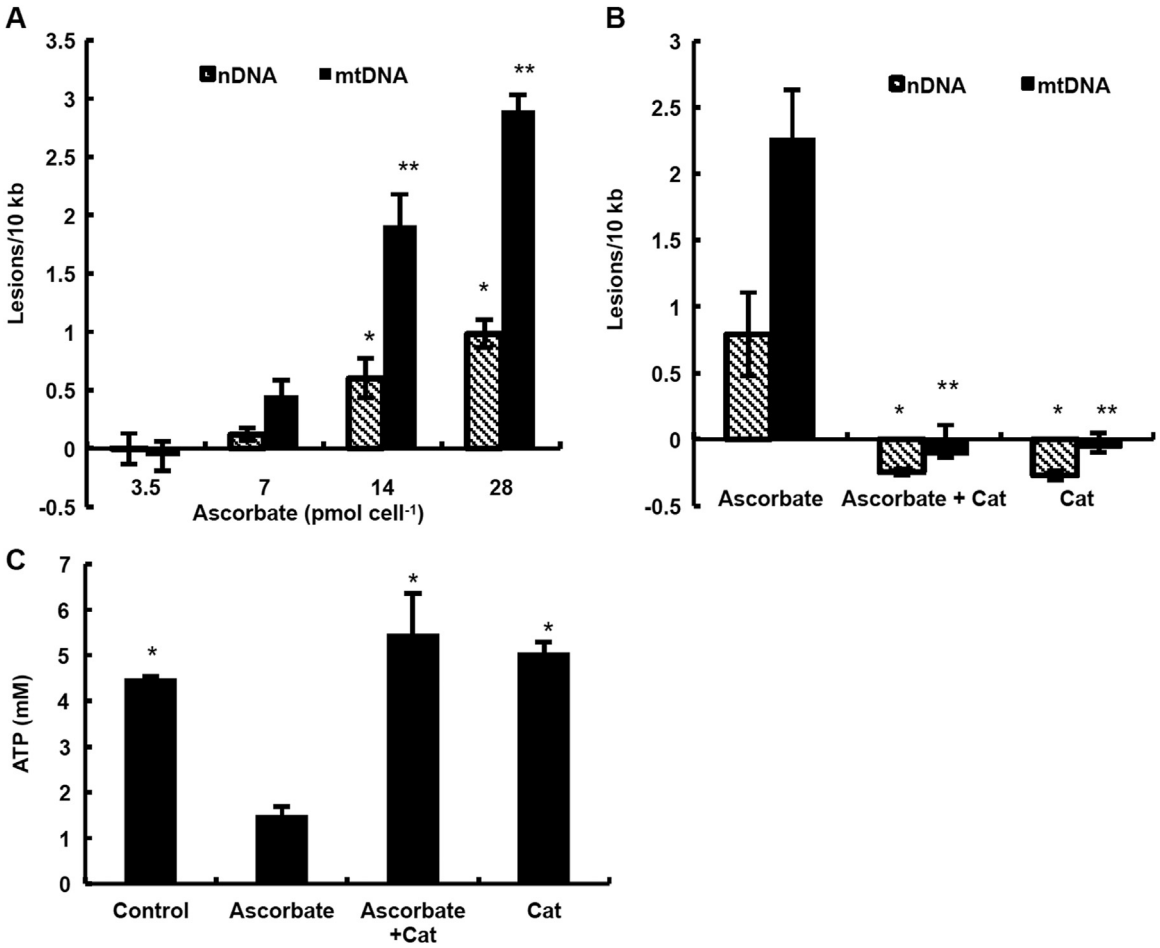

Fig. 7. H_2O_2 generated by ascorbate induces damage to nDNA and mtDNA in MIA PaCa-2 cells and depletes intracellular ATP. (A) MIA PaCa-2 cells were treated with ascorbate (3.5–28 pmol cell^{-1}) for 1 h and then the frequency of DNA lesions was quantified with QPCR. Ascorbate treatment caused dose-dependent damage to nDNA and mtDNA (for nDNA: n =4, mean ± SEM, * $p < 0.05$ *vs.* 3.5 pmol cell^{-1}; for mtDNA: n =8, mean ± SEM, ** $p < 0.001$ *vs.* 3.5 pmol cell^{-1}). **(B)** MIA PaCa-2 cells were incubated with ascorbate (14 pmol cell^{-1}), or ascorbate (14 pmol cell^{-1}) and bovine catalase (200 units mL^{-1}), or bovine catalase (200 units mL^{-1}) alone for 1 h. QPCR analysis revealed no DNA damage from ascorbate when catalase is present in the medium indicating that the DNA damage is caused by H_2O_2 (nDNA: n =4; mean ± SEM; * $p < 0.01$ *vs.* ascorbate; mtDNA: n =4; mean ± SEM; ** $p < 0.001$ *vs.* ascorbate). **(C)** MIA PaCa-2 cells were treated with ascorbate (14 pmol cell^{-1}), combination of ascorbate (14 pmol cell^{-1}) and bovine catalase (200 units mL^{-1}), or bovine catalase (200 units mL^{-1}) for 1 h and then intracellular ATP was determined. ATP was depleted upon treatment with ascorbate, but was unchanged when catalase was present in the medium (n =4; mean ± SEM; * $p < 0.001$ *vs.* P-AscH$^-$).

quantitative dosing metric (mol cell^{-1}) that we previously established for direct-acting compounds that form covalent and tight-binding complexes with their target molecule, we were able to compare the absolute dose that was lethal to 50% of cells (ED_{50}) across five different pancreatic cancer cell lines, without ambiguity resulting from the physical conditions at which the experiments were carried out (Fig. 4) [48]. We observed the k_{cell} for removal of H_2O_2 across the pancreatic cancer cell lines directly correlated with their sensitivity to P-AscH$^-$ (as measured by the ED_{50}) (Fig. 5A). Our data support previous studies' findings that catalase is the major contributor to the removal of high fluxes of H_2O_2 in tumor cells. We observed that both increasing and decreasing the catalase activity had a significant effect on the rate constant of H_2O_2 removal and further investigated whether similar manipulation of basal catalase activity would affect the cells' sensitivity to P-AscH$^-$.

Increasing the catalase activity within the same cell line (MIA PaCa-2) increased resistance to P-AscH$^-$ (Fig. 5B). Many differences exist between cell lines of both the same and different tissue origin; this result supports the contribution of catalase activity in protecting cells from P-AscH$^-$ and limits the other confounding factors that may be present across the different cell lines.

Decreasing catalase activity increased sensitivity to P-AscH$^-$ (Fig. 6). This suggests that catalase may serve as a therapeutic target; a pharmacological inhibitor of catalase activity in tumor cells may be an effective combination therapy to increase the efficacy of P-AscH$^-$. In these studies, we used 3-AT to inhibit catalase. While 3-AT is not currently utilized in the clinic or *in vivo* because it is not specific to tumor cells, there are other natural products that are potential catalase inhibitors currently being investigated. These include: salicylic acid, anthocyanidins, methyldopa, and neutralizing antibodies [65,66]. Thus, advances in targeting these types of reagents may lead to increased efficacy of redox-based therapies and improved patient survival.

There are several targets for oxidative species, *e.g.* H_2O_2. One such target is DNA. Our results support that DNA is a major target of P-AscH$^-$ and that the damage caused to both nuclear and mitochondrial DNA by P-AscH$^-$ is mediated by H_2O_2 (Fig. 7B). mtDNA appears to be more susceptible to oxidative insult than nDNA. This parallels previous reports that show a higher sensitivity of mtDNA to oxidative damage compared to nDNA [67]. These studies looked specifically at H_2O_2 as the oxidant. It has been suggested that this could be due to differences in efficiency of the repair systems of nDNA *vs.* mtDNA [68].

In total, our data provide quantitative evidence that H_2O_2 is involved in the mechanism of P-AscH$^-$ toxicity to cancer cells *in vitro*. The data of Fig. 8 support a similar role for H_2O_2 *in vivo*. P-AscH$^-$ was differentially efficacious in slowing tumor growth in mouse xenografts

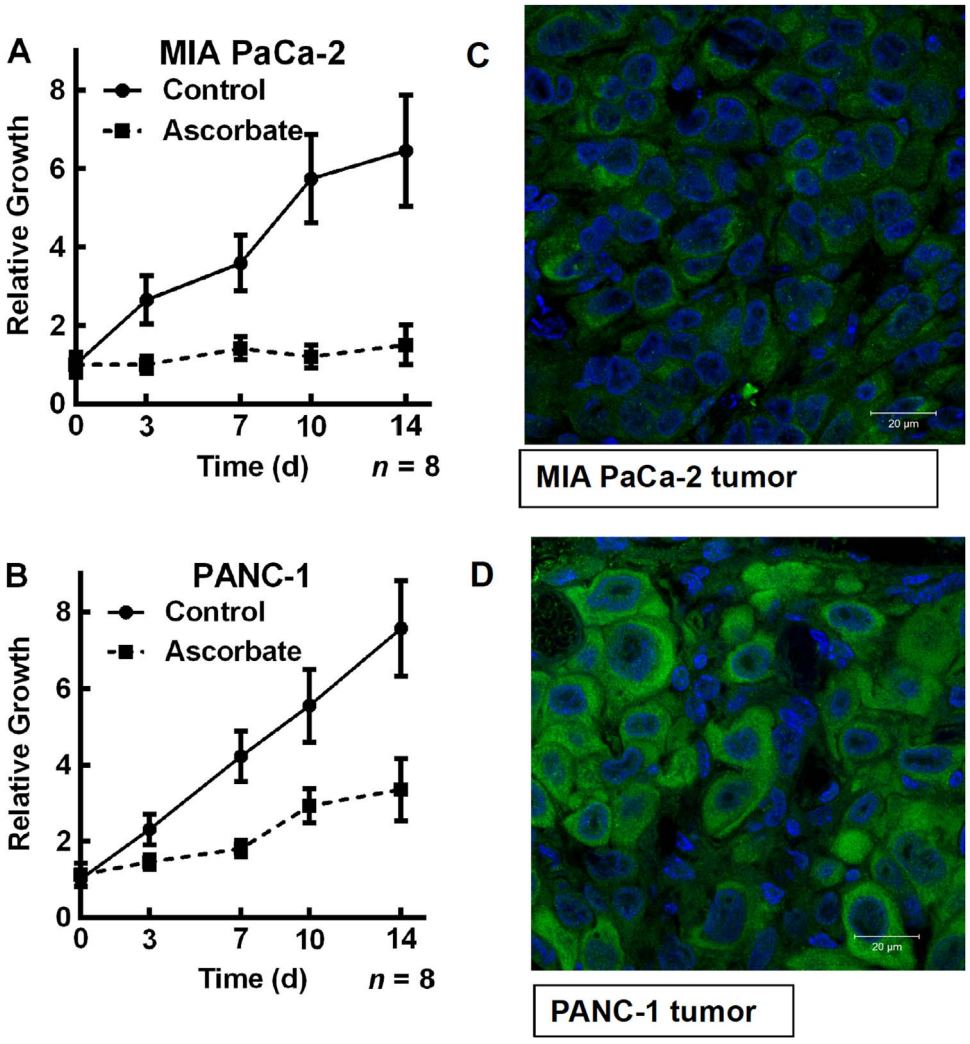

Fig. 8. Pharmacological ascorbate slows growth of MIA PaCa-2 tumors in comparison to PANC-1 tumors *in vivo*. **(A)** MIA PaCa-2 (k_{cell} =1.1×10^{-12} s^{-1} cell^{-1} L; 101,000 active catalase monomers per cell) cells and **(B)** PANC-1 (k_{cell} =5.1×10^{-12} s^{-1} cell^{-1} L; 459,000 active catalase monomers per cell) cells were injected into mice and formed tumors. Mice were treated with IP ascorbate (4 g/kg) twice daily for two weeks. Tumors were measured on day 3, 7, 10, and 14 following first treatment with ascorbate. P-AscH$^-$ slowed the growth rate of PANC-1 xenograft tumors to 42% of the controls; with MIA PaCa-2 tumor xenografts P-AscH$^-$ slowed growth to just 9% of controls. The ratio of k_{cell}(PANC-1)/k_{cell}(MIA PaCa-2) =4.6; the ratio for the relative growth rates compared to controls is essentially identical, 42%/9% =4.7, a remarkable quantitative comparison. **(C)** MIA PaCa-2 tumor catalase immunofluorescence, and **(D)** PANC-1 tumor catalase immunofluorescence. Tumor samples were fixed with 4% paraformaldehyde at 4 °C, and blocked with 5% goat serum for 30 min at 20 °C. The samples were incubated with catalase antibody (1:50) for 20 h at 4 °C. An Alexa Fluor 488 nm goat anti-Rabbit (1:200) was used as secondary antibody. DAPI was used to stain the cell nuclei. The samples were examined using a Zeiss confocal microscope. Scale bar, 20 μm. Tissue samples for PANC-1-derived tumors show considerably more immunofluorescence due to the presence of catalase enzyme than tissue samples from MIA PaCa-2 tumors. (Normalized fluorescent intensity of PANC-1 *vs.* MIA PaCA-2 is 100 ± 27 *vs.* 2.0 ± 0.5.).

of two different pancreatic cancer cell types with quite different capacities to remove H_2O_2: MIA PaCa-2 (k_{cell} =1.1×10^{-12} s^{-1} cell^{-1} L); and PANC-1 (k_{cell} =5.1×10^{-12} s^{-1} cell^{-1} L). P-AscH$^-$ slowed the growth rate of PANC-1 xenograft tumors to 42% of the controls; with MIA PaCa-2 tumor xenografts P-AscH$^-$ slowed growth to just 9% of controls. The ratio of k_{cell}(PANC-1)/k_{cell}(MIA PaCa-2) =4.6; the ratio for the relative growth rates compared to controls is essentially identical, 42%/9% =4.7. This quantitative comparison strongly supports the role of H_2O_2 and catalase in the toxicity that can be induced by P-AscH$^-$. The strong correlation between the capacity of different pancreatic cancer cells to remove H_2O_2 and their sensitivity to P-AscH$^-$ suggests that *in vivo* measurement of catalase activity in tumors may predict which cancers will respond best to P-AscH$^-$ therapy.

This information can also be used in finding combination therapies that may increase the efficacy of treatment for those tumors with higher catalase activities. For example, manganoporphyrins increase the flux of H_2O_2 generated from P-AscH$^-$ when used in combination [4]. They have been shown to be synergistic with P-AscH$^-$ in *in vitro* and *in vivo* animal studies [4]. For tumor cells that have an increased capacity to remove H_2O_2, combinations with agents that increase the flux of H_2O_2 (*e.g.* manganoporphyrins) may be of benefit.

Because P-AscH$^-$ can compromise intracellular ATP levels and induce oxidative DNA damage, it may serve as synergistic adjuvant for those anticancer therapies that have DNA damage as part of their mechanism of action. P-AscH$^-$ has been shown to be synergistic with ionizing radiation [52], a biophysical therapy that induces DNA damage, as well as with gemcitabine [8], an agent that hinders DNA synthesis and antagonizes its repair [69].

5. Conclusions

In this study, we observed that the differential sensitivity to P-AscH$^-$ across pancreatic cancer cells was strongly correlated with their individual capacities to remove H_2O_2. We conclude that:

1. At high doses, ascorbate is oxidized in cell culture medium to

generate a flux of H_2O_2.
2. The rate constants for removal of extracellular H_2O_2 are on average 2-fold higher in normal cells than in cancer cells.
3. The catalase activity of tumor cell lines of varying tissue origin revealed a wide differential in the ability of cells to remove H_2O_2.
4. The ED_{50} of P-AscH$^-$ correlated with the ability of tumor cells to remove extracellular H_2O_2.
5. The response to P-AscH$^-$ in murine-models of pancreatic cancer paralleled the *in vitro* results when these same cells were exposed to P-AscH$^-$.

This work provides definitive evidence that H_2O_2 is involved in the mechanism of P-AscH$^-$ toxicity to cancer cells and that catalase activity is critical in removing this H_2O_2. These results indicate that an *in vivo* measurement of catalase activity in tumors may predict which cancers will respond to pharmacological ascorbate therapy. This information can also be used in finding combination therapies that may increase the efficacy of treatment for those tumors with higher catalase activities.

Author contributions

GRB, CMD, VB, JGW, and BAW designed and executed experiments; CMD, VB, BAW, JGW, JJC, and GRB analyzed the data; CMD and GRB wrote the manuscript with VB, and BAW providing specific text and editorial suggestions; all authors contributed to editing of the work.

Acknowledgments

The authors declare that there are no competing interests. This publication was supported by the National Institutes of Health (NIH), grants R01 CA169046, R01 GM073929, T32 CA148062, P42 ES013661, P30 ES005605, R01 CA184051, and The Gateway for Cancer Research. The ESR Facility at The University of Iowa provided invaluable support. Core facilities were supported in part by the Holden Comprehensive Cancer Center, P30 CA086862. We thank Susan Tsai, MD of the Medical College of Wisconsin for the 339 and 403 cell lines. The content is solely the responsibility of the authors and does not represent views of the National Institutes of Health.

Appendix A. Supplementary material

Supplementary data associated with this article can be found in the online version at http://dx.doi.org/10.1016/j.redox.2016.10.010.

References

[1] Q. Chen, M.G. Espey, M.C. Krishna, J.B. Mitchell, C.P. Corpe, G.R. Buettner, E. Shacter, M. Levine, Ascorbic acid at pharmacologic concentrations selectively kills cancer cells: ascorbic acid as a pro-drug for hydrogen peroxide delivery to tissues, Proc. Natl. Acad. Sci. USA 102 (2005) 13604–13609 (PMID: 16157892).
[2] Q. Chen, M.G. Espey, A.Y. Sun, J.H. Lee, M.C. Krishna, E. Shacter, P.L. Choyke, C. Pooput, K.L. Kirk, G.R. Buettner, M. Levine, Ascorbic acid in pharmacologic concentrations: a pro-drug for selective delivery of ascorbate radical and hydrogen peroxide to extracellular fluid *in vivo*, Proc. Natl. Acad. Sci. USA 104 (2007) 8749–8754 (PMID: 17502596).
[3] J. Du, S.M. Martin, M. Levine, B.A. Wagner, G.R. Buettner, S.H. Wang, A.F. Taghiyev, C. Du, C.M. Knudson, J.J. Cullen, Mechanisms of ascorbate-induced cytotoxicity in pancreatic cancer, Clin. Cancer Res. 16 (2) (2010) 509–520 (PMID: 20068072).
[4] M. Rawal, S.R. Schroeder, B.A. Wagner, C.M. Cushing, J. Welsh, A.M. Button, J. Du, Z.A. Sibenaller, G.R. Buettner, J.J. Cullen, Manganoporphyrins increase ascorbate-induced cytotoxicity by enhancing H_2O_2 generation, Cancer Res. 73 (16) (2013) 5232–5241 (PMID: 23764544).
[5] P. Sestili, G. Brandi, L. Brambilla, F. Cattabeni, O. Cantoni, Hydrogen peroxide mediates the killing of U937 tumor cells elicited by pharmacologically attainable concentrations of ascorbic acid: cell death prevention by extracellular catalase or catalase from cocultured erythrocytes or fibroblasts, J. Pharm. Exp. Ther. 277 (3) (1996) 1719–1725 (PMID: 8667243).
[6] Q. Chen, M.G. Espey, A.Y. Sun, C. Pooput, K.L. Kirk, M.C. Krishna, D.B. Khosh, J. Drisko, M. Levine, Pharmacologic doses of ascorbate act as a prooxidant and decrease growth of aggressive tumor xenografts in mice, Proc. Natl. Acad. Sci. USA 32 (105) (2008) 11105–11109 (PMID: 18678913).
[7] J. Tian, D.M. Peehl, S.J. Knox, Metalloporphyrin synergizes with ascorbic acid to inhibit cancer cell growth through fenton chemistry, Cancer Biother. Radiopharm. 25 (4) (2010) 439–448 (PMID: 20735206).
[8] M.G. Espey, P. Chen, B. Chalmers, J. Drisko, A.Y. Sun, M. Levine, Q. Chen, Pharmacologic ascorbate synergizes with gemcitabine in preclinical models of pancreatic cancer, Free Radic. Biol. Med. 50 (11) (2011) 1610–1619 (PMID: 21402145).
[9] E. Ranzato, S. Biffo, B. Burlando, Selective ascorbate toxicity in malignant *mes*othelioma: a redox Trojan mechanism, Am. J. Respir. Cell Mol. Biol. 44 (1) (2011) 108–117 (PMID: 20203294).
[10] P. Chen, J. Yu, B. Chalmers, J. Drisko, J. Yang, B. Li, Q. Chen, Pharmacological ascorbate induces cytotoxicity in prostate cancer cells through ATP depletion and induction of autophagy, Anticancer Drugs 23 (4) (2012) 437–444 (PMID: 22205155).
[11] C. Klingelhoeffer, U. Kämmerer, M. Koospal, B. Mühling, M. Schneider, M. Kapp, A. Kübler, C.T. Germer, C. Otto, Natural resistance to ascorbic acid induced oxidative stress is mainly mediated by catalase activity in human cancer cells and catalase-silencing sensitizes to oxidative stress, BMC Complement. Alter. Med. 12 (61) (2012) (PMID: 22551313).
[12] A.N. Shatzer, M.G. Espey, M. Chavez, H. Tu, M. Levine, J.I. Cohen, Ascorbic acid kills Epstein-Barr virus positive Burkitt lymphoma cells and Epstein-Barr virus transformed B-cells in vitro, but not in vivo, Leuk. Lymphoma 54 (5) (2013) 1069–1078 (PMID: 23067008).
[13] Y. Ma, J. Chapman, M. Levine, K. Polireddy, J. Drisko, Q. Chen, High-dose parenteral ascorbate enhanced chemosensitivity of ovarian cancer and reduced toxicity of chemotherapy, Sci. Transl. Med. 6 (222) (2014) 222ra18 (PMID: 24500406).
[14] C.S. Cho, S. Lee, G.T. Lee, H.A. Woo, E.J. Choi, S.G. Rhee, Irreversible inactivation of glutathione peroxidase 1 and reversible inactivation of peroxiredoxin II by H_2O_2 in red blood cells, Antioxid. Redox Signal. 12 (11) (2010) 1235–1246 (PMID: 2007018).
[15] J. Du, J.J. Cullen, G.R. Buettner, Ascorbic acid: chemistry, biology and the treatment of cancer, Biochim. Biophys. Acta: Rev. Cancer 1826 (2012) 443–457 (PMID: 22728050).
[16] R.M. Johnson, Yu.D.-Y. HoY-S, F.A. Kuypers, Y. Ravindranath, G.W. Goyette, The effects of disruption of genes for peroxiredoxin-2, glutathione peroxidase-1, and catalase on erythrocyte oxidative metabolism, Free Radic. Biol. Med. 48 (2010) 519–525 (PMID: 19969073).
[17] R. Benfeitas, G. Selvaggio, F. Antunes, P.M. Coelho, A. Salvador, Hydrogen peroxide metabolism and sensing in human erythrocytes: a validated kinetic model and reappraisal of the role of peroxiredoxin II, Free Radic. Biol. Med. 74 (2014) 35–49 (PMID: 24952139).
[18] P. Nicholls, Activity of catalase in the red cell, Biochim Biophys. Acta 99 (1965) 286–297 (PMID: 14336065).
[19] G. Cohen, P. Hochstein, Glutathione peroxidase: the primary agent for the elimination of hydrogen peroxide in erythrocytes, Biochemistry 2 (1963) 1420–1428 (PMID: 14093920).
[20] D.P. Jones, L. Eklöw, H. Thor, S. Orrenius, Metabolism of hydrogen peroxide in isolated hepatocytes: relative contributions of catalase and glutathione peroxidase in decomposition of endogenously generated H_2O_2, Arch. Biochem. Biophys. 210 (2) (1981) 505–516 (PMID: 7305340).
[21] N. Makino, Y. Mochizuki, S. Bannai, Y. Sugita, Kinetic studies on the removal of extracellular hydrogen peroxide by cultured fibroblasts, J. Biol. Chem. 269 (2) (1994) 1020–1025 (PMID: 8288557).
[22] K. Sasaki, S. Bannai, N. Makino, Kinetics of hydrogen peroxide elimination by human umbilical vein endothelial cells in culture, Biochim. Biophys. Acta 1380 (2) (1998) 275–288 (PMID: 9565698).
[23] C.C. Winterbourn, Reconciling the chemistry and biology of reactive oxygen species, Nat. Chem. Biol. 4 (5) (2008) 278–286 (PMID: 18421291).
[24] N. Makino, K. Sasaki, K. Hashida, Y. Sakakura, A metabolic model describing the H_2O_2 elimination by mammalian cells including H_2O_2 permeation through cytoplasmic and peroxisomal membranes: comparisons with experimental data, Biochim. Biophys. Acta 1673 (2004) 149–159 (PMID: 15279886).
[25] P.A. Mitozo, L.F. de Souza, G. Loch-Neckel, S. Flesch, A.F. Maris, C.P. Figueiredo, A.R. Dos Santos, M. Farina, A.L. Dafre, A study of the relative importance of the peroxiredoxin-, catalase-, and glutathione-dependent systems in neural peroxide metabolism, Free Radic. Biol. Med. 51 (1) (2011) 69–77 (PMID: 21440059).
[26] R.M. Johnson, G. Goyette Jr, Y. Ravindranath, Y.S. Ho, Hemoglobin autoxidation and regulation of endogenous H_2O_2 levels in erythrocytes, Free Radic. Biol. Med. 39 (11) (2005) 1407–1417 (PMID: 16274876).
[27] C. De Duve, P. Baudhuin, Peroxisomes (microbodies and related particles), Physiol. Rev. 46 (2) (1966) 323–357 (PMID: 5325972).
[28] S.L. Marklund, N.G. Westman, E. Lundgreen, G. Roos, Copper- and zinc-containing superoxide dismutase, catalase, and glutathione peroxidase in normal and neoplastic cell lines and normal human tissues, Cancer Res. 42 (1982) 1955–1961 (PMID: 7066906).
[29] T.D. Oberley, L.W. Oberley, Antioxidant enzyme levels in cancer, Histol. Histopathol. 12 (1997) 525–535 (PMID: 9151141).
[30] L.W. Oberley, G.R. Buettner, The role of superoxide dismutase in cancer: a review, Cancer Res. 39 (1979) 1141–1149 (PMID: 217531).
[31] I. Roy, N.P. Zimmerman, A.C. Mackinnon, S. Tsai, D.B. Evans, M.B. Dwinell, CXCL12 chemokine expression suppresses human pancreatic cancer growth and metastasis, PLoS One 9 (3) (2014) e90400 (PMID: 24594697).
[32] J. Du, J.A. Cieslak 3rd, J.L. Welsh, Z.A. Sibenaller, B.G. Allen, B.A. Wagner,

A.L. Kalen, C.M. Doskey, R.K. Strother, A.M. Button, S.L. Mott, B. Smith, S. Tsai, J. Mezhir, P.C. Goswami, D.R. Spitz, G.R. Buettner, J.J. Cullen, Pharmacological ascorbate radiosensitizes pancreatic cancer, Cancer Res. 75 (16) (2015) 3314–3326 (PMID: 26081808).
[33] B.A. Wagner, J.R. Witmer, T.J. van 't Erve, G.R. Buettner, An assay for the rate of removal of extracellular hydrogen peroxide by cells, Redox Biol. 1 (2013) 210–217 (PMID: 23936757).
[34] H. Aebi, Catalase *in vitro*, Methods Enzym. 105 (1984) 121–126 (PMID: 6727660).
[35] R. Bonnichsen, Blood catalase, Methods Enzym. 2 (1955) 781–784.
[36] T. Higashi, T. Peters Jr., Studies of rat liver catalase. I. Combined immunochemical and enzymatic determination of catalase in liver cell fractions, J. Biol. Chem. 238 (1963) 3945–3951 (PMID: 14086728).
[37] H. Sies, T. Bücher, N. Oshino, B. Chance, Heme occupancy of catalase in hemoglobin-free perfused rat liver and of isolated rat liver catalase, Arch. Biochem. Biophys. 154 (1) (1973) 106–116 (PMID: 4689773).
[38] B. Chance, H. Sies, A. Boveris, Hydroperoxide metabolism in mammalian organs, Physiol. Rev. 59 (3) (1979) 527–605 (PMID: 37532).
[39] A. Furda, J.H. Santos, J.N. Meyer, B. Van Houten, Quantitative PCR-based measurement of nuclear and mitochondrial DNA damage and repair in mammalian cells, Methods Mol. Biol. 1105 (2014) 419–437 (PMID: 24623245).
[40] B. Van Houten, S. Cheng, Y. Chen, Measuring gene-specific nucleotide excision repair in human cells using quantitative amplification of long targets from nanogram quantities of DNA, Mutat. Res. 460 (2) (2000) 81–94 (PMID: 10882849).
[41] J.J. Salazar, B. Van Houten, Preferential mitochondrial DNA injury caused by glucose oxidase as a steady generator of hydrogen peroxide in human fibroblasts, Mutat. Res. 385 (2) (1997) 139–149 (PMID: 9447235).
[42] D.M. Euhus, C. Hudd, M.C. LaRegina, F.E. Johnson, Tumor measurement in the nude mouse, J. Surg. Oncol. 31 (4) (1986) 229–234 (PMID: 3724177).
[43] B.A. Wagner, S. Venkataraman, G.R. Buettner, The rate of oxygen utilization by cells, Free Radic. Biol. Med 51 (2011) 700–712 (PMID: 21664270).
[44] M.P. Murphy, How mitochondria produce reactive oxygen species, Biochem J. 417 (1) (2009) 1–13 (PMID: 19061483).
[45] K.E. Olney, J. Du, T.J. van 't Erve, J.R. Witmer, Z.A. Sibenaller, B.A. Wagner, G.R. Buettner, J.J. Cullen, Inhibitors of hydroperoxide metabolism enhance ascorbate-induced cytotoxicity, Free Radic. Res 47 (3) (2013) 154–163 (PMID: 23205739).
[46] G.R. Buettner, C.F. Ng, M. Wang, V.G.J. Rodgers, F.Q. Schafer, A new paradigm: manganese superoxide dismutase influences the production of H_2O_2 in cells and thereby their biological state, Free Radic. Biol. Med. 41 (2006) 1338–1350 (PMID: 17015180).
[47] C. De Duve, The separation and characterization of subcellular particles, Harvey Lect. 59 (1965) 49–87 (PMID: 5337823).
[48] C.M. Doskey, T.J. van 't Erve, B.A. Wagner, G.R. Buettner, Moles of a substance per cell is a highly informative dosing metric in cell culture, PLoS One 10 (7) (2015) e0132572 (PMID: 26172833).
[49] D.R. Spitz, J.H. Elwell, Y. Sun, L.W. Oberley, T.D. Oberley, S.J. Sullivan, R.J. Roberts, Oxygen toxicity in control and H_2O_2-resistant Chinese hamster fibroblast cell lines, Arch. Biochem Biophys. 279 (1990) 249–260 (PMID:2350176).
[50] M. Gülden, A. Jess, J. Kammann, E. Maser, H. Seibert, Cytotoxic potency of H_2O_2 in cell cultures: impact of cell concentration and exposure time, Free Radic. Biol. Med 49 (2010) 1298–1305 (PMID: 20673847).
[51] M.C. Sobotta, A.G. Barata, U. Schmidt, S. Mueller, G. Millonig, T.P. Dick, Exposing cells to H_2O_2: a quantitative comparison between continuous low-dose and one-time high-dose treatments, Free Radic. Biol. Med. 60 (2013) 325–335 (PMID: 23485584).
[52] J. Du, J.A. Cieslak 3rd, J.L. Welsh, Z.A. Sibenaller, B.G. Allen, B.A. Wagner, A.L. Kalen, C.M. Doskey, R.K. Strother, A.M. Button, S.L. Mott, B. Smith, S. Tsai, J. Mezhir, P.C. Goswami, D.R. Spitz, G.R. Buettner, J.J. Cullen, Pharmacological ascorbate radiosensitizes pancreatic cancer, Cancer Res. 75 (16) (2015) 3314–3326 (PMID: 26081808).
[53] D.S. Martin, J.R. Bertino, J.A. Koutcher, ATP depletion + pyrimidine depletion can markedly enhance cancer therapy: fresh insight for a new approach, Cancer Res. 60 (24) (2000) 6776–6783 (PMID: 11156364).
[54] W.X. Zong, D. Ditsworth, D.E. Bauer, Z.Q. Wang, C.B. Thompson, Alkylating DNA damage stimulates a regulated form of necrotic cell death, Genes Dev. 18 (11) (2004) 1272–1282. http://dx.doi.org/10.1101/gad.1199904 (PMID: 15145826).
[55] P.M. Herst, K.W. Broadley, J.L. Harper, M.J. McConnell, Pharmacological concentrations of ascorbate radiosensitize glioblastoma multiforme primary cells by increasing oxidative DNA damage and inhibiting G2/M arrest, Free Radic. Biol. Med. 52 (8) (2012) 1486–1493 (PMID: 22342518).
[56] M.L. Castro, M.J. McConnell, P.M. Herst, Radiosensitisation by pharmacological ascorbate in glioblastoma multiforme cells, human glial cells, and HUVECs depends on their antioxidant and DNA repair capabilities and is not cancer specific, Free Radic. Biol. Med. 74 (2014) 200–209 (PMID: 24992837).
[57] J.A. Cieslak, R.K. Strother, M. Rawal, J. Du, C.M. Doskey, S.R. Schroeder, A. Button, B.A. Wagner, G.R. Buettner, J.J. Cullen, Manganoporphyrins and ascorbate enhance gemcitabine cytotoxicity in pancreatic cancer, Free Radic. Biol. Med. 83 (2015) 227–237 (PMID: 25725418).
[58] M. Uetaki, S. Tabata, F. Nakasuka, T. Soga, M. Tomita, Metabolomic alterations in human cancer cells by vitamin C-induced oxidative stress, Sci. Rep. 5 (2015) 13896 (PMID: 26350063).
[59] J. Yun, E. Mullarky, C. Lu, Bosch, A. Kavalier, K. Rivera, J. Roper, I.I.C. Chio, E.G. Giannopoulou, C. Rago, A. Muley, J.M. Asara, J. Paik, O. Elemento, Z. Chen, D.J. Pappin, L.E. Dow, N. Papadopoulos, S.S. Gross, L.C. Cantley, Vitamin C selectively kills *KRAS* and *BRAF* mutant colorectal cancer cells by targeting GAPDH, Science 350 (6266) (2015) 1391–1396 (PMID: 26541605).
[60] J. Du, B.A. Wagner, G.R. Buettner, J.J. Cullen, The role of labile iron in the toxicity of pharmacological ascorbate, Free Radic. Biol. Med. 84 (2015) 289–295 (PMID: 25857216).
[61] M. Mojić, J. Bogdanović Pristov, D. Maksimović-Ivanić, D.R. Jones, M. Stanić, S. Mijatović, I. Spasojević, Extracellular iron diminishes anticancer effects of vitamin C: an in vitro study, Sci. Rep. 4 (2014) 5955 (PMID: 25092529).
[62] F.Q. Schafer, G.R. Buettner, Redox state of the cell as viewed though the glutathione disulfide/glutathione couple, Free Radic. Biol. Med. 30 (2001) 1191–1212 (PMID: 11368918).
[63] J.L. Welsh, B.A. Wagner, T.J. van 't Erve, P.S. Zehr, D.J. Berg, T.R. Halfdanarson, N.S. Yee, K.L. Bodeker, J. Du, L.J. Roberts 2nd, J. Drisko, M. Levine, G.R. Buettner, J.J. Cullen, Pharmacological ascorbate with gemcitabine for the control of metastatic and node-positive pancreatic cancer (PACMAN): results from a phase I clinical trial, Cancer Chemother. Pharmacol. 71 (3) (2013) 765–775. http://dx.doi.org/10.1007/s00280-013-2070-8 (PMID: 23381814).
[64] J. Cullen, D. Berg, J. Buatti, G. Buettner, M. Smith, C. Anderson, W. Sun, B. Allen, W. Rockey, D. Spitz, B. Wagner, S. Schroeder, R. HohlGemcitabine, ascorbate, and radiation therapy for pancreatic cancer, Phase 1, at The University of Iowa, (Start date 01/2014) (NCT01852890) ⟨http://clinicaltrials.gov/ct2/show/NCT01852890⟩
[65] K. Scheit, G. Bauer, Direct and indirect inactivation of tumor cell protective catalase by salicylic acid and anthocyanidins reactivated intracellular ROS signaling and allows for synergistic effects, Carcinogenesis 36 (3) (2015) 400–411 (PMID: 25653236).
[66] K. Scheit, G. Bauer, Synergistic effects between catalase inhibitors and modulators of nitric oxide metabolism on tumor cell apoptosis, Anticancer Res. 34 (2014) 5337–5350 (PMID: 25275027).
[67] F.M. Yakes, B. Van Houten, Mitochondrial DNA damage is more extensive and persists longer than nuclear DNA damage in human cells following oxidative stress, Proc. Natl. Acad. Sci. USA 94 (2) (1997) 514–519 (PMID: 9012815).
[68] S.D. Cline, Mitochondrial DNA damage and its consequences for mitochondrial gene expression, Biochim. Biophys. Acta 1819 (9–10) (2012) 979–991 (PMID: 22728831).
[69] E. Mini, S. Nobili, B. Caciagli, I. Landini, T. Mazzei, Cellular pharmacology of gemcitabine, Ann. Oncol. 17 (Suppl 5) (2016) v7–v12 (PMID: 16807468).